Inorg. Chem. **2002**, *41*, 7136–7142

Methyloxorhenium(V) Complexes with Two Bidentate Ligands: Syntheses and Reactivity Studies

Xiaopeng Shan, Arkady Ellern, and James H. Espenson*

Ames Laboratory and the Department of Chemistry, Iowa State University of Science and Technology, Ames, Iowa 50011

Received August 14, 2002

Four new methyloxorhenium(V) complexes were synthesized: $MeReO(PA)_2$ (**1**), $MeReO(HQ)_2$ (**2**), $MeReO(MQ)_2$ (**3**), and MeReO(diphenylphosphinobenzoate)$_2$ (**4**) (in which PAH = 2-picolinic acid, HQH = 8-hydroxyquinoline, and MQH = 8-mercaptoquinoline). Although only one geometric structure has been identified crystallographically for **1**, **2**, and **3**, two isomers of **3** and **4** in solution were detected by NMR spectroscopy. These compounds catalyze the sulfoxidation of thioethers by pyridine *N*-oxides and sulfoxides. The rate law for the reaction between pyridine *N*-oxides and thioethers, catalyzed by **1**, shows a first-order dependence on the concentrations of pyridine *N*-oxide and **1**. The second-order rate constants of a series of para-substituted pyridine *N*-oxides fall in the range of 0.27–7.5 L mol^{-1} s^{-1}. Correlation of these rate constants by the Hammett LFER method gave a large negative reaction constant, $\rho = -5.2$. The next and rapid step does not influence the kinetics, but it could be explored with competition experiments carried out with a pair of methyl aryl sulfides, $MeSC_6H_4$-*p*-Y. The value of each rate was expressed relative to the reference compound that has Y = H. A Hammett analysis of k_Y/k_H gave $\rho = -1.9$. Oxygen-18 labeled **1** was used in a single turnover experiment for 4-picoline *N*-oxide and dimethyl sulfide. No ^{18}O-labeled DMSO was found. We suggest that the reaction proceeds by way of two intermediates that were not observed during the reaction. The first intermediate contains an opened PA-chelate ring; this allows the pyridine *N*-oxide to access the primary coordination sphere of rhenium. The second intermediate is a *cis*-dioxorhenium(VII) species, which the thioether then attacks. Oxygen-18 experiments were used to show that the two oxygens of this intermediate are not equivalent; only the new oxygen is attacked by, and transferred to, SR_2. Water inhibits the reaction because it hydrolyzes the rhenium(VII) intermediate.

Introduction

Certain aspects of the coordination chemistry of rhenium have been widely developed because of the radiotherapeutic applications of the β-emitting isotopes ^{186}Re and ^{188}Re.[1−3] Most of these rhenium complexes contain a $\{Re^{V}O\}$ core.[4−7] Often a monoanionic bidentate ligand is present. Typical donor atom pairs such as P,O (HPO = phosphinocarboxylic acid),[8,9] N,O (HNO = e.g., picolinic acid or 8-hydroxyquinoline),[10−13] and N,S (HNS = 2-mercaptoquinoline) were used.[12] Molybdenum complexes have been extensively investigated owing to interest in their oxotransferase activity.[14−18] In comparison, only a few rhenium complexes have been investigated.[19−23] This research focuses on

* Author to whom correspondence should be addressed. E-mail: espenson@iastate.edu.

(1) Blower, P. J.; Prakash, S. *Perspect. Bioinorg. Chem.* **1999**, *4*, 91−143.
(2) Hashimoto, K.; Yoshihara, K. *Top. Curr. Chem.* **1996**, *176*, 275−291.
(3) Blaeuenstein, P. *New J. Chem.* **1990**, *14*, 405−407.
(4) Bandoli, G.; Tisato, F.; Refosco, F.; Gerber, T. I. A. *Rev. Inorg. Chem.* **1999**, *19*, 187−210.
(5) Romão, C. C.; Kühn, F. E.; Herrmann, W. A. *Chem. Rev.* **1997**, *97*, 3197−3246.
(6) Herrmann, W. A.; Kuehn, F. E. *Acc. Chem. Res.* **1997**, *30*, 169−180.
(7) Herrmann, W. A. *J. Organomet. Chem.* **1986**, *300*, 111−137.
(8) Correia, J. D. G.; Domingos, A.; Santos, I.; Bolzati, C.; Refosco, F.; Tisato, F. *Inorg. Chim. Acta* **2001**, *315*, 213−219.
(9) Bolzati, C.; Tisato, F.; Refosco, F.; Bandoli, G.; Dolmella, A. *Inorg. Chem.* **1996**, *35*, 6221−6229.
(10) Harris, T. A.; McKinney, T. M.; Wu, W.; Fanwick, P. E.; Walton, R. A. *Polyhedron* **1996**, *15*, 3289−3298.
(11) Dorsett, T. E.; Walton, R. A. *J. Organomet. Chem.* **1976**, *114*, 127−134.
(12) Leeaphon, M.; Rohl, K.; Thomas, R. J.; Fanwick, P. E.; Walton, R. A. *Inorg. Chem.* **1993**, *32*, 5562−5568.
(13) Wilcox, B. E.; Heeg, M. J.; Deutsch, E. *Inorg. Chem.* **1984**, *23*, 2962−2967.
(14) Coucouvanis, D. *Acc. Chem. Res.* **1991**, *24*, 1−8.
(15) Holm, R. H.; Berg, J. M. *Acc. Chem. Res.* **1986**, *19*, 363−370.
(16) Holm, R. H. *Coord. Chem. Rev.* **1990**, *100*, 183−221.

10.1021/ic025952f CCC: $22.00
Published on Web 11/15/2002

Chart 1. Structural Formulas of [2 + 2] Methyloxorhenium(V) Compounds

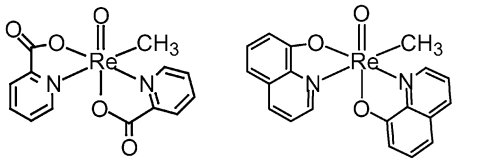

MeReO(PA)$_2$ **1**

MeReO(HQ)$_2$ **2**

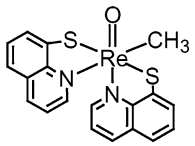

MeReO(MQ)$_2$

3a

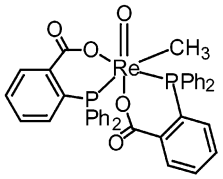

MeReO(diphenylphosphinobenzoate)$_2$ **4a**

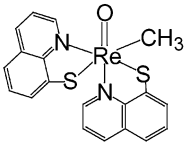

MeReO(MQ)$_2$

3b

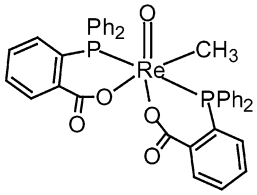

MeReO(diphenylphosphinobenzoate)$_2$ **4b**

compounds containing a methyloxorhenium(V) core, {MeRe^{v}O}.[24−27]

We have now extended our exploration of rhenium catalysts[28−33] by the preparation and characterization of four new [2 + 2] methyloxorhenium compounds, Chart 1. These reactions are catalyzed by the following:

$$RSR' + XC_5H_4NO \xrightarrow{[Re]} RS(O)R' + C_5H_4N \quad (1)$$

$$R_2S + R'_2S(O) \rightleftharpoons R_2S(O) + R'_2S \quad (2)$$

Kinetic studies were carried out with **1**, the most effective catalyst. Our goal has been to identify the steps in the mechanism, including the formulation of chemically reasonable reaction intermediates. This includes the trapping of a transient dioxorhenium(VII) species.

Experimental Section

Reagents and Instrumentation. Methyltrioxorhenium(VII), CH_3ReO_3 or MTO, was prepared from sodium perrhenate, tetramethyl tin, and chlorotrimethylsilane.[34] The chelating ligands were purchased from commercial sources and used as received. Anhydrous methylene chloride was the solvent for UV−vis spectrophotometry. D_1-chloroform for NMR studies was dried over 4 Å molecular sieves (Fisher) for 24 h at 200 °C.

UV−vis data were obtained with a Shimadzu model 2501 spectrophotometer. Least-squares kinetic fits were carried out with KaleidaGraph software. Bruker DRX-400 MHz and AC200 spectrometers were used to record ^{1}H, ^{13}C, and ^{31}P NMR spectra. The chemical shift for ^{1}H was defined relative to that of the residual $CHCl_3$ in the solvent, δ 7.27 ppm. Infrared spectra were recorded by a Nicolet-500 spectrometer. GC−MS spectra were recorded by a Finnegan MAT MAGNUM mass spectrometer. Elemental analysis was performed by Desert Analytics Laboratory.

Syntheses. Compounds **1**−**3** were prepared from MTO (50 mg, 0.2 mmol), the bidentate ligand (0.4 mmol), and the reducing agent triphenylphosphine (53 mg, 0.2 mmol) in 20 mL of CH_2Cl_2. After the mixture was stirred for 12 h, 20 mL of hexanes was layered on the top of the resulting solution, and the mixture was placed in a freezer at ca. −12 °C. After 24 h, a black powder had deposited; it was filtered and rinsed with hexanes. A crystal suitable for X-ray diffraction analysis was obtained by recrystallization from methylene chloride−hexanes. Dimethyl sulfide (19 mg, 0.3 mmol) could also be used as the reducing agent for the preparation of **1** provided that anhydrous sodium sulfate was added as a drying agent to complete the reaction. If the acidic form of the monoanionic ligand is written as H(X,Y), where X and Y are the donor atoms, the chemical equation for the syntheses is

$$MeReO_3 + 2H(X,Y) + PPh_3/Me_2S \rightarrow MeRe(O)(X,Y)_2 + H_2O + Ph_3PO/Me_2SO \quad (3)$$

1 was obtained in 83% yield from triphenylphosphine and in 53% yield from dimethyl sulfide. ^{1}H NMR: δ 8.84 (d, 1H), 8.52 (d, 1H), 8.44 (m, 1H), 8.29 (m, 1H), 8.19 (d, 1H), 7.77 (m, 3H), 4.43 (s, 3H). ^{13}C NMR: 180, 163, 153, 150, 148, 146, 143, 130, 126, 125, 53, 29, 11. IR ($CHCl_3$): 1002.85 cm^{-1} and for the ^{18}O-labeled compound, 950.75 cm^{-1}. The two agree precisely with the predicted $(18:16)^{1/2}$ ratio. UV−vis ($CHCl_3$) λ_{max}, nm (log ϵ): 568 (2.3), 396.5 (3.83), 260 (4.14). Anal. $C_{13}H_{11}N_2O_5Re$: found (calcd) C, 33.85 (33.84); H, 2.48 (2.40); N, 6.06 (6.07).

2 was obtained in 80% yield. ^{1}H NMR: δ 8.56 (d, 1H), 8.36 (m, 1H), 8.21 (m, 1H), 7.66 (m, 4H), 7.40 (m, 3H), 7.07 (d, 1H), 6.46 (d, 1H), 4.53 (s, 3H). ^{13}C NMR: too insoluble. IR ($CHCl_3$): 979.86 cm^{-1}. UV−vis ($CHCl_3$) λ_{max}, nm (log ϵ): 470 (sh), 417 (3.70), 360 (sh). Anal. $C_{19}H_{15}N_2O_3Re$: found (calcd): C, 44.64 (45.14); H, 2.92 (2.99); N, 5.29 (5.54).

3 was obtained in 50% yield. Two sets of ^{1}H NMR resonance peaks were found in solution with a ratio of 3:1. Two geometric

(17) Thapper, A.; Lorber, C.; Fryxelius, J.; Behrens, A.; Nordlander, E. *J. Inorg. Biochem.* **2000**, *79*, 67−74.
(18) Young, C. G. *J. Biol. Inorg. Chem.* **1997**, *2*, 8810−816.
(19) Arias, J.; Newlands, C. R.; Abu-Omar, M. M. *Inorg. Chem.* **2001**, *40*, 2185−2192.
(20) Huang, R.; Espenson, J. H. *J. Mol. Catal.* **2001**, *168*, 39−46.
(21) Arterburn, J. B.; Perry, M. C. *Org. Lett.* **1999**, *1*, 769−771.
(22) Abu-Omar, M. M.; Khan, S. I. *Inorg. Chem.* **1998**, *37*, 4979−4985.
(23) Arterburn, J. B.; Nelson, S. L. *J. Org. Chem.* **1996**, *61*, 2260−2261.
(24) Espenson, J. H.; Shan, X.; Wang, Y.; Huang, R.; Lahti, D. W.; Dixon, J.; Lente, G.; Ellern, A.; Guzei, I. A. *Inorg. Chem.* **2002**, *41*, 2583−2591.
(25) Jacob, J.; Guzei, I. A.; Espenson, J. H. *Inorg. Chem.* **1999**, *38*, 3266−3267.
(26) Jacob, J.; Guzei, I. A.; Espenson, J. H. *Inorg. Chem.* **1999**, *38*, 1040−1041.
(27) Lente, G.; Shan, X.; Guzei, I. A.; Espenson, J. H. *Inorg. Chem.* **2000**, *39*, 3572−3576.
(28) Jacob, J.; Lente, G.; Guzei, I. A.; Espenson, J. H. *Inorg. Chem.* **1999**, *38*, 3762−3763.
(29) Lente, G.; Guzei, I. A.; Espenson, J. H. *Inorg. Chem.* **2000**, *39*, 1311−1319.
(30) Lente, G.; Jacob, J.; Guzei, I. A.; Espenson, J. H. *Inorg. React. Mech.* **2000**, *2*, 169−177.
(31) Lente, G.; Espenson, J. H. *Inorg. Chem.* **2000**, *39*, 4809−4814.
(32) Wang, Y.; Espenson, J. H. *Inorg. Chem.* **2002**, *41*, 2266−2274.
(33) Wang, Y.; Espenson, J. H. *Org. Lett.* **2000**, *2*, 3525−3526.
(34) Herrmann, W. A.; Kratzer, R. M.; Fischer, R. W. *Angew. Chem., Int. Ed. Engl.* **1997**, *36*, 2652−2654.

isomers were assigned to these peaks according to the X-ray structure and an earlier study of pyridine exchange reactions.[35] In solution, the major species is **3a**. ^{1}H NMR: δ 10.88 (d, 1H), 8.39 (d, 1H), 8.34 (d, 2H), 8.06 (d, 1H), 7.80 (t, 1H), 7.74 (d, 1H), 7.58 (m, 1H), 7.74 (d, 1H), 7.41 (t, 1H), 6.95 (d, 1H), 6.75 (m, 1H), 4.95 (s, 3H). The minor solution species is **3b**. Only three peaks are available because of broadening and overlap with peaks from **3a**. ^{1}H NMR: δ 9.40 (s, 1H), 8.65 (s, 1H), 5.14 (s, 3H). ^{13}C NMR: too insoluble. IR ($CHCl_3$): **3a**, 985.46 cm^{-1}; **3b**, 998.96 cm^{-1}. UV−vis ($CHCl_3$) λ_{max}, nm (log ϵ): 699 (2.6), 432 (3.78), 267.5 (4.43). Anal. $C_{19}H_{15}N_2ORe S_2$: found (calcd): C, 42.16 (42.44); H, 2.54 (2.81); N, 5.13 (5.21); S, 11.37 (11.93).

4 was prepared by adding MTO (50 mg, 0.2 mmol) into 20 mL of CH_2Cl_2 containing 2-diphenylphosphinobenzoic acid (184 mg, 0.6 mmol), which served both as the reducing agent and as the new ligand. The color of the solution changed to violet. After 12 h of being stirred, the mixture was layered with hexanes and put into the freezer. A dark powder was isolated by filtration 24 h later and rinsed with hexanes. It consisted of two geometric isomers, **4a** and **4b**, in a total yield of 65%. The two could not be separated, but their NMR spectra in $CDCl_3$ were resolved and assigned as explained later. **4a** ^{1}H NMR: d 6.5−8.5 (m, 14H), 3.39 (t, 3H); ^{31}P NMR: −0.34 (d, J_{PP} = 9 Hz), −3.07 (d, J_{PP} = 9 Hz). **4b** ^{1}H NMR: 6.5−8.5 (m, 14H), 4.12 (t, 3H); ^{31}P NMR: 6.64 (d, J_{PP} = 262 Hz), −5.28 (d, J_{PP} = 262 Hz).

X-ray Studies. Crystals for **1**, **2**, and **3a** were selected under ambient conditions. Each crystal was mounted and centered in the X-ray beam by use of a video camera. The crystal evaluation and data collection were performed on a Bruker CCD-1000 diffractometer with Mo Kα (λ = 0.71073 Å) radiation and a detector-to-crystal distance of 4.98 cm. The initial cell constants were obtained from three series of ω scans at different starting angles. Each series consisted of 30 frames collected at intervals of 0.3° in a 10° range about ω with the exposure time of 10 s per frame. The reflections were successfully indexed by an automated indexing routine built into the SMART program. The final cell constants were calculated from a set of strong reflections from the actual data collection. The data were collected using the full-sphere routine for high redundancy. The data were corrected for Lorentz and polarization effects. The absorption correction was based on fitting a function to the empirical transmission surface as sampled by multiple equivalent measurements[36] using SADABS software.[37]

The position of the heavy atom was found by the Patterson method. The remaining atoms were located in an alternating series of least-squares cycles and difference Fourier maps. All non-hydrogen atoms were refined in full-matrix and isotropic approximation. All hydrogen atoms were placed at calculated idealized positions and were allowed to ride on the neighboring atoms with relative isotropic displacement coefficients. The ORTEP diagrams were drawn at 50% probability level.

Kinetics. Reactions of pyridine *N*-oxides and dimethyl sulfide were monitored by following the decrease in absorbance from 275 to 310 nm according to which pyridine *N*-oxide was being studied. Owing to the large values of their molar absorptivities, a cell with a path length of 0.05 cm in a cylindrical cell holder thermostated at 25.0 ± 0.2 °C was used. Dimethyl sulfide was added in at least 10-fold excess, allowing the absorbance-time data to be fitted to pseudo-first-order kinetics, according to eq 2:

$$\mathrm{Abs}_t = \mathrm{Abs}_\infty + (\mathrm{Abs}_0 - \mathrm{Abs}_\infty) \times \exp(-k_{obs}t) \qquad (4)$$

Competition Kinetics. A different aspect of the reaction scheme was studied by this method. A pair of methyl aryl sulfides with different para substituents at concentrations 10 times higher than that of 4-picoline *N*-oxide were used. The concentrations of the two starting sulfides and of the sulfoxides formed were determined by NMR spectroscopy 15 min after the beginning of the reaction. The rate constant ratio for $MeSC_6H_4Y$ as compared to MeSPh is given simply as the product of two concentration ratios at a given time because the sulfide concentrations are nearly invariant during the initial reaction period.

$$\frac{k_Y}{k_H} = \frac{\mathrm{d[MeS(O)C_6H_4Y]}/\mathrm{d}t}{\mathrm{d[MeS(O)Ph]}/\mathrm{d}t} = \frac{[\mathrm{MeS(O)C_6H_4Y}]_t}{[\mathrm{MeS(O)Ph}]_t}\frac{[\mathrm{MeSPh}]_0}{[\mathrm{MeSC_6H_4Y}]_0} \qquad (5)$$

Oxygen-18 Labeling. Equilibration between MTO and 30 times the molar ratio of $H_2{}^{18}O$ (90% enrichment) was allowed to proceed for 20 min in anhydrous methylene chloride, which was sufficient for oxygen exchange between MTO and water.[38] The resulting solution was vacuum-dried. The same procedure was repeated three times, yielding a sample of $MeRe^{18}O_3$ enriched to ca. 50% ^{18}O content. It was used to prepare **1** by the PPh_3 method. The ^{18}O content of **1** was ca. 50% by IR spectroscopy. A reaction was carried out in anhydrous methylene chloride with 4-picoline *N*-oxide (10 mM), dimethyl sulfide (20 mM), and **1** (10 mM) to guarantee the formation of enough sulfoxides. The isotopic content of the resulting solution was determined by GC−MS.

Table 1. Experimental Data for the X-ray Diffraction Studies of **1**, **2**, and **3a**

	1	**2**	**3a**
empirical formula	$C_{13}H_{11}N_2O_5Re$	$C_{19}H_{15}N_2O_3Re$	$C_{19}H_{15}N_2ORe S_2$
fw	461.44	505.53	537.65
a, Å	28.466(7)	9.233(2)	8.4428(14)
b, Å	7.0933(17)	9.724(2)	9.1357(15)
c, Å	15.186(4)	10.780(2)	12.531(2)
α, deg		101.054(3)	85.504(3)
β, deg	111.892(4)	103.955(3)	89.214(3)
γ, deg		112.402(4)	64.825(3)
V, Å^3	2845.3(12)	823.8(3)	871.8(3)
Z	8	2	2
space group	*C*2/*c*	$P\bar{1}$	$P\bar{1}$
T, K	298(2)	298(2)	298(2)
wavelength, Å	0.71073	0.71073	0.71073
ρ_{calcd}, g cm^{-3}	2.154	2.038	2.048
μ, mm^{-1}	8.564	7.396	7.218
R indices (all data)[a]	R1 = 0.0821, wR2 = 0.1686	R1 = 0.0354, wR2 = 0.0832	R1 = 0.0681, wR2 = 0.1566

[a] $R1 = \sum||F_o| - |F_c||/\sum|F_o|$; $wR2 = \{\sum[w(F_o^2 - F_c^2)^2]/\sum[w(F_o^2)^2]\}^{1/2}$.

Results

Structures. Table 1 shows the crystallographic parameters for **1**, **2**, and **3a**, and Figure 1 displays their molecular structures drawn by the program CrystalMaker.[39] In all three compounds the rhenium(V) atom occupies the center of a distorted octahedron defined by its axial ligands, the terminal

(35) Espenson, J. H.; Shan, X.; Lahti, D. W.; Rockey, T. M.; Saha, B.; Ellern, A. *Inorg. Chem.* **2001**, *40*, 6717−6724.
(36) Blessing, R. H. *Acta Crystallogr., Sect. A* **1995**, *51*, 33−38.
(37) All software and sources of the scattering factors are contained in the SHELXTL (version 5.1) program library (Sheldrick, G. M. *SHELXTL*, Version 5.1; Bruker Analytical X-ray Systems: Madison, WI, 1997).
(38) Herrmann, W. A.; Kuchler, J. G.; Weichselbaumer, G.; Herdtweck, E.; Kiprof, P. *J. Organomet. Chem.* **1989**, *372*, 351−370.
(39) Palmer, D. *CrystalMaker*, 2nd ed.; Hollywell Press: Bicester, Oxfordshire, England, 1999.

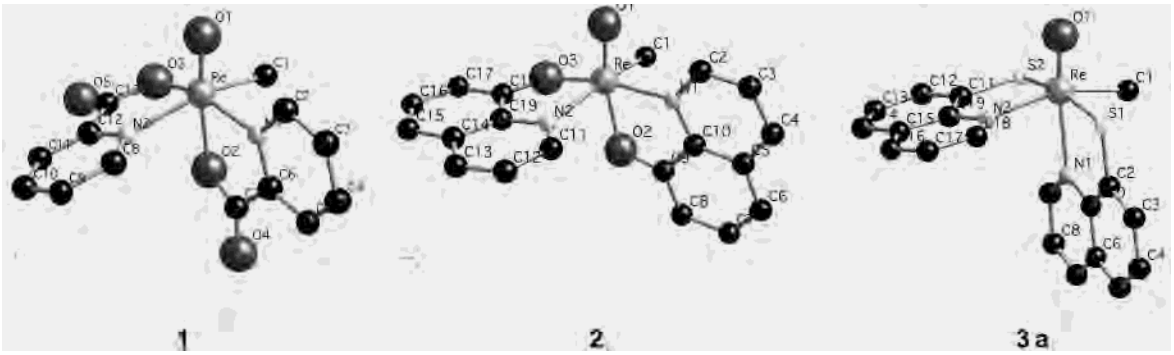

Figure 1. Crystallographically determined molecular structures of compounds **1**, **2**, and **3a**. Table 2 shows the selected bond lengths and angles.

Table 2. Selected Bond Lengths (pm) and Angles[a] (deg) of **1**, **2**, and **3a** Complexes

	1	**2**	**3a**
Re−O(1)	166.2(8)	167.7(4)	167.4(8)
Re−C(1)	211.1(13)	211.1(6)	211.3(12)
Re−N(1)	211.3(9)	212.5(4)	238.3(9)
Re−N(2)	216.3(9)	220.1(4)	214.8(9)
Re−O(2)	210.0(7)	203.7(4)	
Re−O(3)	201.4(8)	198.6(4)	
Re−S(1)			244.7(3)
Re−S(2)			231.3(3)
O(1)−Re−C(1)	98.8(5)	97.9(3)	102.5(4)
O(1)−Re−N(1)	90.9(4)	87.47(17)	165.6(4)
O(1)−Re−N(2)	103.9(4)	99.02(17)	103.6(4)
C(1)−Re−N(1)	88.6(5)	89.3(2)	78.8(4)
C(1)−Re−N(2)	156.3(4)	81.66(15)	153.6(4)
N(2)−Re−N(1)	97.9(3)	100.12(16)	76.9(3)
O(1)−Re−O(2)	*165.3(4)*	*162.86(17)*	
N(1)−Re−O(3)	159.4(4)	166.48(15)	
C(1)−Re−O(2)	84.1(5)	84.8(2)	
S(1)−Re−N(2)			95.9(3)
S(1)−Re−S(2)			165.66(10)
C(1)−Re−S(2)			87.2(4)

[a] Italicized entries: *trans*[oxo-Re-donor atom] angles.

oxo group, and one donor atom of one bidentate ligand. The three remaining donor atoms and the methyl group occupy the equatorial plane. Table 2 lists the important bond distances and angles. In all of these compounds the Re≡O distances are virtually identical at 167 pm, as are the Re−C distances at 211 pm. The values of ν(Re−O) from the IR studies fall in the range of 985−1003 cm^{-1} for **1**−**4**, relatively insensitive to the ligand environment. In every case, the donor atom trans to the terminal oxo group lies at a longer distance than its counterpart in the equatorial plane; this comes as no surprise, reflecting extensive π back-bonding from oxo to rhenium(V). In keeping with that, the trans(O≡Re-donor atom) angles lie in the range of 162.9−165.5°, notably less than 180°.

All of **1**−**4** should exist as four geometrical isomers. No evidence for structures of **1** or **2**, other than the ones characterized, was obtained. Even the solution NMR in deuterated chloroform from the original preparation prior to product isolation showed the single isomer. Two isomers in ca. 3:1 ratio were found for **3** in solution, but only the major one, **3a**, was isolated. The minor isomer, **3b**, is characterized by δ(Me-Re) 5.14. The hydrogen signals from the MQ ligand are somewhat broadened, which is not the case for **3a** or free MQH. This suggests an internal process and brings to mind the exchange between Py and five-coordinate MeReO(edt)Py (edtH$_2$ = 1,2-ethane dithiol). For it, the transition state is six-coordinate and features a turnstile rotation that interchanges the Me group and the two Py ligands.[35,40] Such an exchange, if it occurs within **3b**, could well give rise to signal broadening.

Compound **4** exists as ca. equimolar amounts of two isomers, the structures of which are presented in Chart 1. The basis for these assignments is the widely different coupling constants in the ^{31}P NMR spectra. J_{P-P} = 9 Hz in **4a** and 262 Hz in **4b**. According to the literature,[41−43] the very high coupling constant suggests a structure for **4b** in which the two phosphorus donor atoms lie trans to one another.

The donor atoms are N and O for PA and HQ; we surmise that the heterocyclic nitrogen is the more weakly bound when both are equatorial; consequently **1** and **2** adopt structures with an axial O-donor atom. Whatever atom is trans to the oxo group is the most weakly bound of all, irrespective of the inherent Lewis basicity. The same rule applies to ligand MQ, which gives rise to the minor isomer **3b**, because a thiolate sulfur is a better Lewis base than a ring nitrogen. In that sense, **3a** is similar insofar as the MQ ligand that spans an axial and an equatorial position. The two isomers differ only in regards to the orientation of the in-plane ligand, which may be a factor of less consequence. Again, the two isomers of **4** differ in the same way as do the two isomers of **3**. Both isomers of **4** have an O-donor atom trans to the oxo group; that donor is a weaker Lewis base than a phosphine toward Re(V). The comparable abundances of **4a** and **4b** may reflect the steric influence of the bulky phosphine ligand.

Oxygen Atom Transfer: Sulfoxide to Sulfide. The following nearly isoenergetic reaction[19] occurred when any of the compounds **1**−**4** were used in catalytic quantity with a 10-fold excess of dimethyl sulfide:

$$Ph_2SO + Me_2S \rightarrow Ph_2S + Me_2SO \qquad (6)$$

Unlike some oxorhenium(V) compounds that catalyze this reaction efficiently, such as [(hoz)$_2$Re(O)(OH$_2$)][OTf][19] and

(40) Lahti, D. W.; Espenson, J. H. *J. Am. Chem. Soc.* **2001**, *123*, 6014−6024.
(41) Bennett, M. A.; Robertson, G. B.; Rokicki, A.; Wickramasinghe, W. A. *J. Am. Chem. Soc.* **1988**, *110*, 7098−7105.
(42) Cotton, F. A.; Dikarev, E. V.; Herrero, S. *Inorg. Chem.* **2000**, *39*, 609−616.
(43) Cowan, R. L.; Trogler, W. C. *J. Am. Chem. Soc.* **1989**, *111*, 4750−4761.

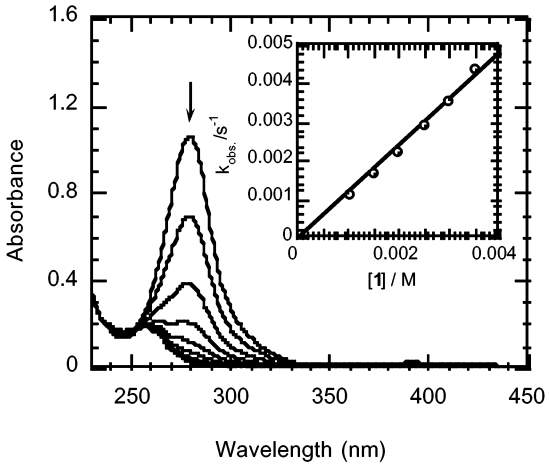

Figure 2. Repetitive scans of 10 mM 4-picoline *N*-oxide, 100 mM dimethyl sulfide, and 2 mM **1** in anhydrous methylene chloride at 25 °C. The inset shows the plot of k_{cat} against the concentration of the catalyst.

MeReO(dithiolatte)PPh_3,[32,33] none of these compounds led to a rapid reaction for reasons that will be presented later. We therefore turned our attention to a catalytic system where efficient reactions could be observed.

Oxygen Atom Transfer: Pyridine *N*-Oxides to Thioethers. Kinetic studies of these reactions in anhydrous methylene chloride were carried out:

$$XC_5H_4NO + RSR' \rightarrow XC_5H_4N + RS(O)R' \qquad (7)$$

Studies were limited to catalyst **1** because **2** and **3** react more slowly, and **4** is not available as a single compound. A sample repetitive scan spectrum (X = 4-Me, Me_2S) is presented in Figure 2.

The absorbance-time decrease, which shows the greatest amplitude at 279 nm, follows first-order kinetics. The values of k_{obs} so obtained are linear functions of the total catalyst concentration, designated as $[\mathbf{1}]_T$, to reflect the fact that at various points during the cycle **1** exists in different forms present at low concentrations.

$$-\frac{d[XC_5H_4NO]}{dt} = k_{cat}[XC_5H_4NO][1]_T \qquad (8)$$

The kinetic determinations employed a ≥10-fold excess of sulfide over pyridine *N*-oxide. Varying the sulfide concentration gave the same rate constant, $k_{cat} = 1.23 \pm 0.01$ (100 mM Me_2S) and 1.20 ± 0.05 (10 mM) L mol^{-1} s^{-1} (100 mM Me_2S). Different thioethers also gave the same value of $k_{cat} = 1.20 \pm 0.05$ (Me_2S), 1.22 ± 0.01 (pentamethylene sulfide), and 1.28 ± 0.07 L mol^{-1} s^{-1} (*tert*-butyl methyl sulfide). For a range of pyridine *N*-oxides, the identity of X exerts a strong influence on the value of k_{cat}, as can be seen from Table 3.

Competition Experiments. The foregoing reveals that the sulfide enters the catalytic cycle at a stage later than the step(s) that determine the rate and the value of k_{cat}. That is, RSR′ reacts with an active rhenium intermediate in a fast subsequent step. To evaluate the effects of thioethers it was therefore useful to take the thioethers in pairs, for which purpose $MeSC_6H_4Y$ and MeSPh were employed. The design of the experiment is presented in this diagram:

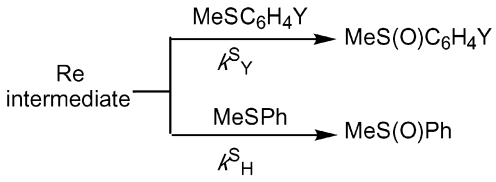

Table 3. Kinetics of Sulfoxidation Reactions Catalyzed by **1**[a]

UV Spectra of XC_5H_4NO and k_{cat}[b]

X	λ_{max}, nm (ϵ/10^4 L mol^{-1} cm^{-1})	k_{cat}, L mol^{-1} s^{-1}
4-MeO	280 (0.415)	7.5
4-Me	279 (1.07)	1.23
2-Me	272 (1.04)	0.57
3-Me	278 (0.920)	0.43
4-Ph	310 (1.54)	0.36
4-H	277 (0.615)	0.27

Relative Rate Constants for **5** and Methyl Aryl Sulfides[c]

Y	k_Y/k_H
4-MeO	5.1
4-Me	2.4
4-H	1.00 (rel)
4-Cl	0.44
4-Br	0.37
4-HO_2C	0.18
4-MeC(O)	0.11
4-CN	0.078

[a] In anhydrous dichloromethane at 25 °C. [b] Conditions: 10 mM XC_5H_4NO, 100 mM Me_2S, and 2−8 mM **1**. [c] At 25 °C in D_1-chloroform with 10 mM 4-MeC_5H_4NO, 2 mM **1**, and 50 mM each of MeSPh and $MeSC_6H_4Y$.

The NMR data were analyzed to determine the ratio k^S_Y/k^S_H for the different aryl groups on sulfide according to eq 5. The second part of Table 3 presents the results of such determinations. For reasons to be presented later, it was deemed essential to determine the same ratio for two other pyridine *N*-oxides. These data are also given in Table 3.

Oxygen-18 Labeling. Stoichiometric amounts of **1** and 4-picoline *N*-oxide and twice as much Me_2S were employed in the case where $MeRe^{18}O(PA)_2$ was employed in anhydrous dichloromethane. The solution was analyzed by GC−MS after 2 h reaction time. Although ample $Me_2S^{16}O$ was detected, $Me_2S^{18}O$ proved absent.

Discussion

Thermochemical and Electronic Considerations. Sulfoxide-to-sulfide transfer of an oxygen atom is nearly isoenergetic;. $\Delta G° = -2.9$ kJ for reaction 6 between diphenyl sulfoxide and dimethyl sulfide in methylene chloride.[19] The use of pyridine *N*-oxides provides a system with a considerably greater driving force. From thermochemical data for C_5H_4NO and Me_2S,[44−47] we estimate $\Delta G° \simeq \Delta H° = -63$ kJ mol^{-1}.

(44) Shaofeng, L.; Pilcher, G. *J. Chem. Thermodyn.* **1988**, *20*, 463−465.
(45) Ribeiro da Silva, M. D. M. C.; Agostinha, M.; Matos, R.; Vaz, M. C.; Santos, L. M. N. B. F.; Pilcher, G.; Acree, W. E., Jr.; Powell, J. R. *J. Chem. Thermodyn.* **1998**, *30*, 869−878.
(46) Jenks, W. S.; Matsunaga, N.; Gordon, M. *J. Org. Chem.* **1996**, *61*, 1275−1283.
(47) Mackle, K. *Tetrahedron* **1963**, *19*, 1159−1170.

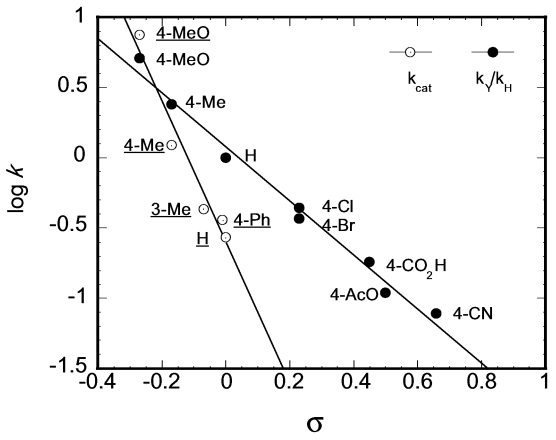

Figure 3. LFER correlations of k_{cat} values for reactions between XC_5H_4NO and 100 mM Me_2S in the presence of 2−8 mM **1** in anhydrous CH_2Cl_2 at 25 °C and of relative rate constants k_Y/k_H determined by competition kinetics for reactions of $MeSC_6H_4Y$ between 10 mM 4-picoline *N*-oxide and 50 mM each of $MeSC_6H_4Y$ and $C_6H_5SCH_3$ in the presence of 2 mM **1** in $CDCl_3$ at 25 °C.

The value of k_{cat} depends strongly on the electronic properties of the substituent on the pyridine *N*-oxide ring. For the five entries in Table 3 with substituents in the 4- and 3-positions, an analysis according to Hammett's method gives $\rho_{cat} = -5.2$ in Figure 3. This is an exceptionally negative value, most reasonably interpreted in terms of two composite effects that enter in the same direction. More will be said about this in what follows.

A similar analysis was carried out on the rate constant ratio k^S_Y/k^S_H. The fact that this quantity is a ratio and not an absolute rate constant does not compromise the answer in the least. From the data in Table 3 we find $\rho_S = -1.9$, as shown in Figure 3.

Substrate Binding. It seems self-evident that activation of a pyridine *N*-oxide requires its coordination to rhenium(V) for the catalyst to exert its effect. In systems studied earlier, this has not appeared to pose a significant part of the overall barrier because five-coordinate catalysts such as MeReO(dithiolate)PPh_3 permit its ready entry. For **1**, however, one must propose either that PyO attacks **1** as it is, giving rise to a seven-coordinate intermediate, or that ring-opening of one arm of one PA ligand precedes entry of PyO. We surmise that the N donor atom is preferentially released to avoid the presumably unfavorable $[Re]^+O^-$ in dichloromethane.

We have argued strongly against any dissociative process for complexes such as MeReO(dithiolate)L.[35,40] Thus, it seems we must also consider direct ligand displacement as the route to **5**. We discount this mechanism, however, because the parent is not a five-coordinate complex from which ligand dissociation becomes unlikely but a six-coordinate one in which the weakness of a rhenium ligand trans to the oxo group has been well-established.

By whichever pathway the **1** = **5** reaction occurs, the net process is an equilibrium that can be represented by an equilibrium constant K_{15}, the value of which varies with the X group of XC_5H_4NO according to its Lewis basicity. Because this step remains at equilibrium, its mechanism, while of intrinsic interest in its own right, remains immaterial in the kinetic analysis. Stronger Lewis bases are more strongly coordinated in **5**, which provides one factor contributing to the negative reaction constant ρ_{cat} found for k_{cat}. That contribution is designated ρ_{15}, and it is one component of ρ_{cat}.

Rate-Controlling Step (RCS). The rate law indicates that the thioether is not involved in the mechanism until after the RCS because the rate remains independent of variations in the concentration and identity of RSR′. We therefore conclude that intermediate **5** undergoes unimolecular cleavage of the N−O bond of coordinated pyridine *N*-oxide:

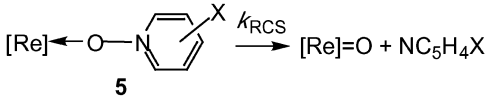

The experimental rate constant k_{cat} is therefore a composite: $k_{cat} = K_{15} \times k_{RCS}$. The large negative reaction constant $\rho_{cat} = -5.2$ allows us to argue that the substituent effects on each component must have the same sign, lest cancellation of the effects take place. Because K_{15} represents a Lewis acid−base equilibrium, ρ_{15} will therefore be negative, as argued previously. The negative reaction constant ρ_{RCS} indicates that electron flow from the oxygen of the coordinate pyridine *N*-oxide provides the principal barrier at the transition state:

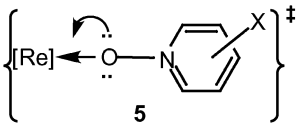

Thioether Step and Its Oxo-Group Selectivity. A direct reaction occurs between intermediate **6** and RSR′. Because it occurs rapidly as compared to the RCS, kinetic competition experiments were employed. The rate constants relative to MeSPh are given in the second part of Table 3. The reaction constant is $\rho_S = -1.9$, which indicates nucleophilic attack of the thioether on one oxygen of dioxorhenium(VII) intermediate **6**. This forms the next intermediate, **7**, that might best be viewed as being or becoming a sulfoxide complex of rhenium(V).

What is astonishing, however, is the high selectivity the thioether exhibits as to which of the two oxo groups of **6** it attacks. Data obtained with the catalyst **1** as $MeRe(^{18}O)(PA)_2$ (oxygen-18 content, 50%) gave, in combination with an equimolar quantity of $4\text{-}MeC_5H_4N^{16}O$ and dimethyl sulfide, only $Me_2S^{16}O$. Had the thioether reacted nonselectively, the enrichment level of the sulfoxide would have corresponded to 25% $Me_2S^{18}O$.

Examination of the plausible structure of **6** is helpful in this regard. As shown in Scheme 1, intermediate **7a** appears to be a dead-end because displacement of sulfoxide by the dangling pyridine arm of PA is impossible. On the other hand, unimolecular displacement within **7b** restores **1** directly and forms $Me_2S^{16}O$ exclusively.

Scheme 1

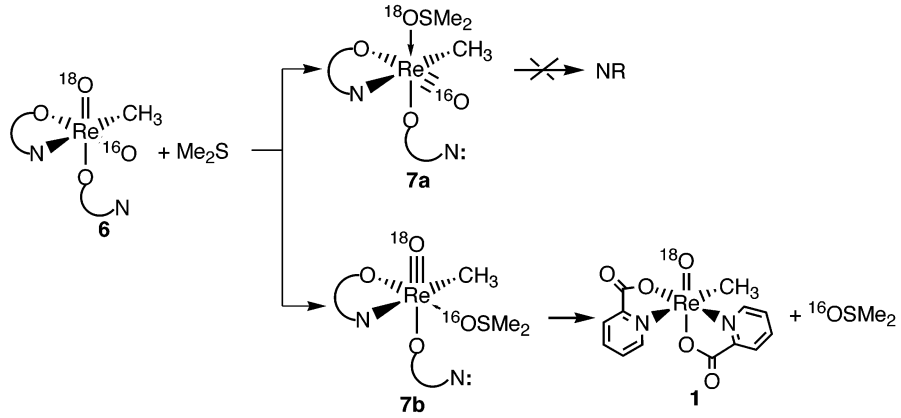

Conclusion

Four new rhenium(V) complexes with monoanionic bidentate ligands (PA, HQ, MQ, and DPPB) were synthesized and characterized. All of them catalyze oxygen atom transfer from milder oxidants, pyridine *N*-oxides or sulfoxides, to thioethers. On the basis of kinetic and mechanistic studies, a multistep mechanism has been proposed with involvement of several unobserved but plausible intermediates to account for the reaction at each stage.

Acknowledgment. This research was supported by the U.S. Department of Energy, Office of Basic Energy Sciences, Division of Chemical Sciences under Contract W-7405-Eng-82.

Supporting Information Available: Crystallographic data for **1**, **2**, and **3a**, including traditional ORTEP diagrams. This material is available free of charge via the Internet at http://pubs.acs.org.

IC025952F